Nanoporous metal/metal-oxide composite prepared by one-step de-alloying AlNiCoYCu metallic glasses

Hao Yang [a, b], Huajun Qiu [c], Jun-Qiang Wang [b, *], Juntao Huo [b], Xinmin Wang [b], Run-Wei Li [b], Jianguo Wang [a, **]

[a] School of Materials Science and Engineering, Anhui University of Technology, Maanshan, Anhui 243032, China
[b] Key Laboratory of Magnetic Materials and Devices & Zhejiang Province Key Laboratory of Magnetic Materials and Application Technology, Ningbo Institute of Materials Technology & Engineering, Chinese Academy of Sciences, Ningbo 315201, China
[c] School of Chemistry and Chemical Engineering, Chongqing University, Chongqing 400044, China

ARTICLE INFO

ABSTRACT

A bicontinuous nanoporous NiCoCuY metal/metal-oxide composite was fabricated by one-step de-alloying $Al_{85-x}Ni_6Y_6Co_3Cu_x$ (x = 1, 3 and 5) metallic glasses in alkaline solutions. The electro-chemical performance of the nanoporous composites as binder-free electrodes has been evaluated. It is found that 3 at.% Cu addition can achieve the largest capacitance which is attributed to the increase in electric conductance. The capacitance of nanoporous composites can reach as high as 1.22 F cm^{-2} if the $Al_{82}Ni_6Y_6Co_3Cu_3$ sample was de-alloyed in 4 M KOH for 50 min. Such a one-step strategy of de-alloying metallic glass not only generates a promising functional material for energy storage, but also provides a facile way for decreasing the resistance of electrode material.

© 2017 Elsevier B.V. All rights reserved.

1. Introduction

Electrochemical capacitances (also called supercapacitors or ultracapacitors) have become one of the promising energy storage devices for next-generation power devices because of their high power density, fast charge/discharge rates, long cycle life, and better cycling stability compared with secondary batteries [1—6]. According to the energy storage mechanisms, electrochemical capacitances can be divided to two types, i.e. (i) double-layer capacitance, which involves non-Faradic process, (ii) faradaic pseudo-capacitance, which is a Faradaic process [7—9]. These two mechanisms can work separately or together, depending on the active electrode materials in electrochemical capacitors [10]. However, the capability of electrode material is significantly influenced by its surface area and morphology. Nanostructured materials hold promising application potentials as electrochemical capacitors because they have high specific surface area for rapid diffusion and fast redox reaction. Recently, nanoporous metals with high specific surface and low density have attracted great attention in many technological application including actuators, catalysis, energy storage and so forth [11—13]. Transition metal oxides, such as CoO, NiO, RuO_2, MnO_2, etc, are superior supercapacitor electrode materials. Electric conductivity is another important factor for the capability of electrode. However, the band gap of transition metal oxides between the conduction band and valence band is relatively narrow, which result in poor electrical conductivity leading to their low capacitance. In current years, two strategies have been developed to overcome this deficiency. The first is the external conductive reinforcements by compositing with conductive materials, such as carbon [14], conducting polymers [15], nanoporous metals [16], and conductive metal oxides [17]. Unfortunately, these reinforcements are often limited by weak oxide/conductor interfaces. The second is internal conductive reinforcements by doping various metal atoms, which is taken advantaged to improve the weak interfaces. For example, Kang et al. [18] obtained a thick Au-doped MnO_2 film by doping the Au atoms in MnO_2 using physical vapor deposition. However, deposition is a complex and slow process.

In this work, we used one-step corrosion strategy to fabricate NiCo-based nanoporous metal/metal-oxide composites by de-

* Corresponding author.
** Corresponding author.
E-mail addresses: jqwang@nimte.ac.cn (J.-Q. Wang), wrcrpp@ahut.edu.cn (J. Wang).

alloying AlNiCo-based metallic glasses. The influence of the concentration of etching solution, corrosion time and alloying of noble metals on the electro-chemical capacitance were studied. Based on this work, the optimal experimental parameters for fabricating the nanoporous composites with large capacitance were determined.

2. Material and methods

The master alloys with nominal composition of $Al_{85-x}Ni_6Y_6Co_3Cu_x$ (x = 1, 3 and 5) (at. %) were prepared by melting highly pure melts (>99.9 wt %) using an induction-melting furnace under the protection of Argon atmosphere. The master alloy was then melt in quartz tube and injected onto a spinning copper roller to prepare metallic glass ribbons. The thickness of the ribbon was about 20−30 μm and the width was about 2 mm. The metallic glass precursor was de-alloyed in KOH aqueous solutions with different concentrations at room temperature. After de-alloying, the samples were rinsed with deionized water and dehydrated alcohol.

The structure of the metallic glass precursor and de-alloyed alloys were characterized by X-ray diffraction using a diffractometer with Cu K_α radiation (Bruker D8 Advance). The microstructures of the de-alloyed samples were characterized by scanning electron microscopy (SEM, Hitachi S-4800). Chemical analysis was performed by energy-dispersive X-ray spectrometer (EDS, Oxford INCA x-sight). Electrochemical tests were carried out at room temperature using an electrochemical workstation (Zahner Zennium) in a three-electrode cell with a Pt foil as counter electrode and Ag/AgCl (Cl^- concentration inside of the electrode is 3.5 M) as the reference electrode. For capacitive performance measurements, the electrolyte is 1 M KOH aqueous solution. The working electrode was the de-alloyed ribbon. The nominal area of the samples immersed into the electrolyte for electrochemical tests was 10 mm^2.

3. Results and discussion

The XRD patterns of the $Al_{85-x}Ni_6Y_6Co_3Cu_x$ (x = 1, 3 and 5) ribbons in Fig. 1a show only a broad diffraction halo without crystalline peaks, confirming the homogenous amorphous structure. The sharp exothermic crystallization peaks in DSC traces further confirms the glassy state of the $Al_{85-x}Ni_6Y_6Co_3Cu_x$ samples, as shown in Fig. 1b. Replacing Al by Cu can enhance the thermal stability which is confirmed by the increase in crystallization temperature (T_x). This is different from that replacing Ni by Cu decrease the thermal stability [19]. The structure of de-alloyed sample was also studied using XRD, as shown in Fig. 1c. After being etched for 1 h, the amorphous hump at $2\theta = 38°$ disappeared, while crystalline peaks appeared. These crystalline peaks were ascribed to Ni(Co,Cu) metal and Y, Ni, Co metal oxides. The crystal size for the dealloyed samples was estimated to be about 3 nm according to the diffraction peak in XRD curves.

To understand the de-alloying process, micro-structure of the cross-section of the ribbon was investigated. Akin to the de-alloyed Ag-Mg-Ca metallic glass [20], the nanoporous layers grew from the two surfaces into the metallic glass precursor, as shown in Fig. 2. Since the ribbon was prepared using a single roller spinning furnace, the cooling rate on the roller-contacted side was much higher than the free side. It is interesting to observe that the de-alloyed layer on the free side is thicker compared to the roller-contacted side. This suggests that the faster-cooled metallic glass has a better corrosion resistance. The linear-scanned EDX curves confirmed that Al in the metallic glass had been mostly removed, since the content of Al decreased after being de-alloyed while the contents of other elements increased.

After de-alloying, the rest Co and Ni can be oxidized/reduced between different valence (Co^{2+}/Ni^{2+} and Co^{3+}/Ni^{3+}) which is

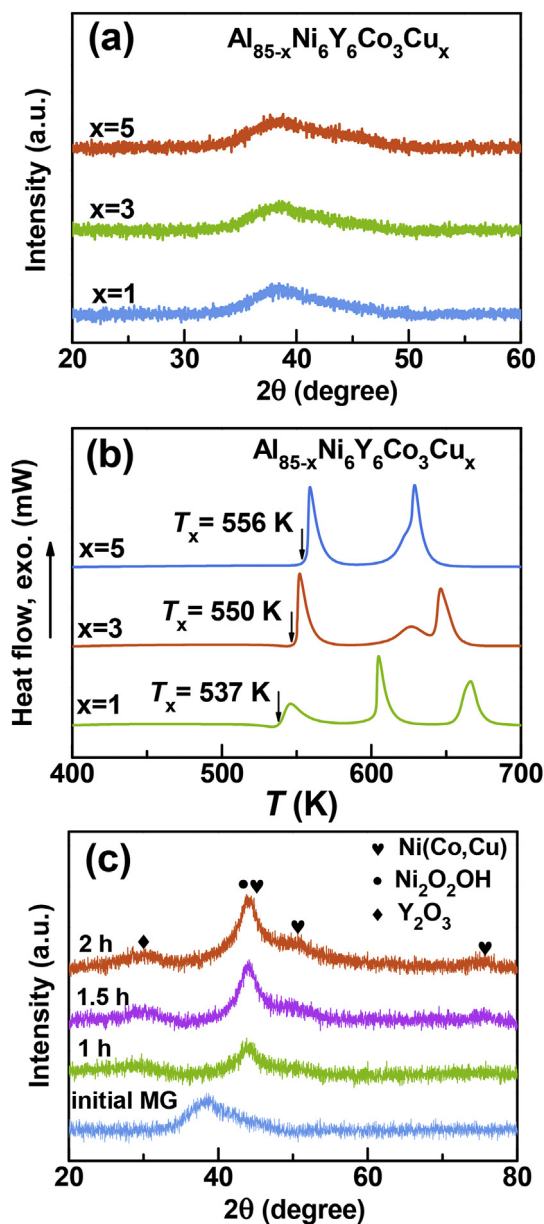**Fig. 1.** (a) XRD curves and (b) DSC traces of the as-spun $Al_{85-x}Ni_6Y_6Co_3Cu_x$ ribbons. (c) XRD curves of the samples dealloyed in 4 M KOH aqueous solution for 1 h, 1.5 h and 2 h.

applied as supercapacitor electrodes. The electrochemical capacitance was examined to evaluate their application potential as binder-free electrodes. It is known that the low electric resistivity of the nanoporous materials can contribute to large capacitance [18]. To obtain a lower electric resistivity, the noble metal Cu is alloyed into the metallic glass. Fig. 3a shows the CV curves of $Al_{85-x}Ni_6Y_6Co_3Cu_x$ (x = 1, 3 and 5) de-alloyed for 50 min in 4 M KOH. On the curves, one can find that the content of copper changes the integral area of the CV curve, but not change the potential of redox peaks. From the galvanostatic charge/discharge (GCD) curves (Fig. 3b) of $Al_{85-x}Ni_6Y_6Co_3Cu_x$ (x = 1, 3, 5) de-alloyed 50 min in 4 M KOH at 6 mA cm^{-2}, it is easy to find that the sample of $Al_{82}Ni_6Y_6Co_3Cu_3$ exhibits the largest discharging time. The areal specific capacitance was calculated from equation C = $I\Delta t/S\Delta V$, where I is the discharge current, Δt is the discharge time, ΔV is the potential range and S is the area of the electrode. The calculation presents
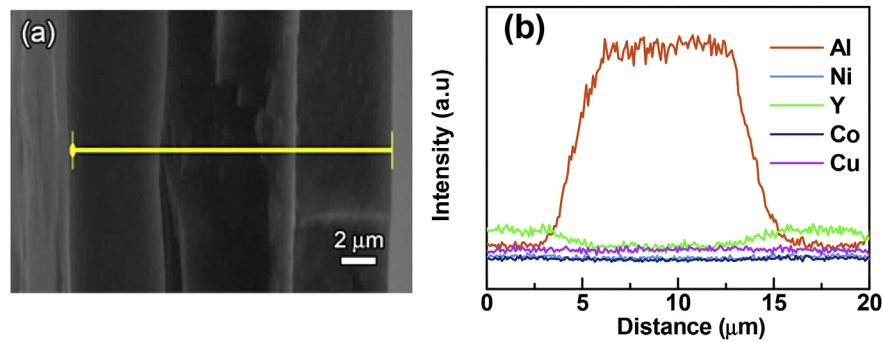
Fig. 2. (a) The SEM micrograph of the cross section of a $Al_{82}Ni_6Y_6Co_3Cu_3$ metallic glass ribbon dealloyed for 40 min and (b) EDX line scan of the cross section.
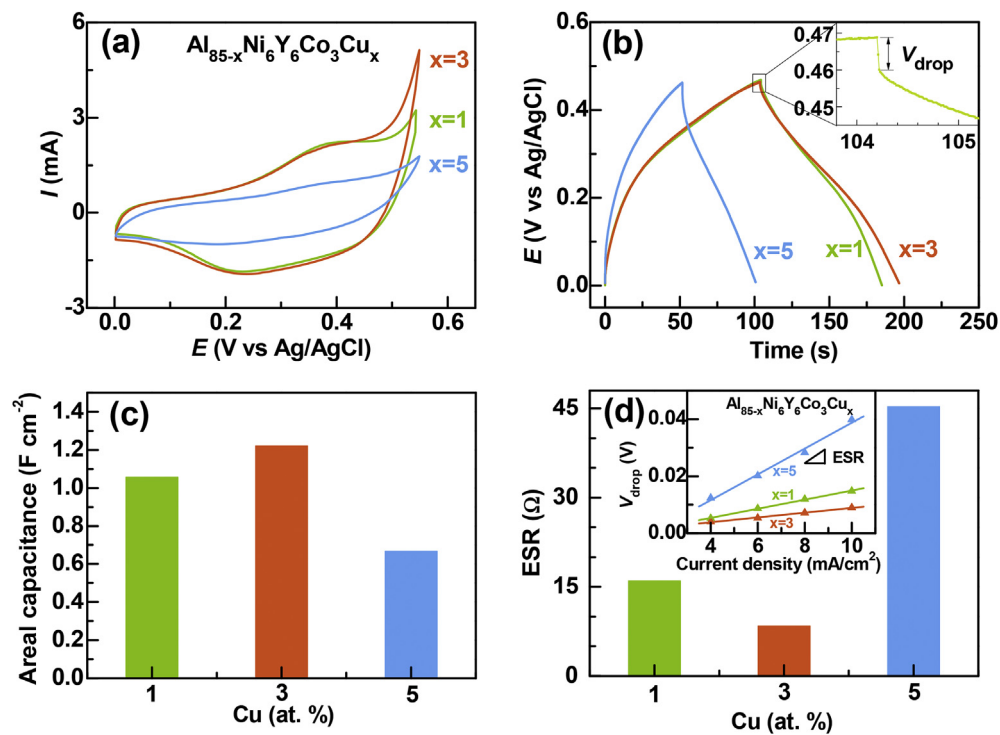

Fig. 3. (a) CV curves of $Al_{85-x}Ni_6Y_6Co_3Cu_x$ (x = 1, 3, 5) dealloyed in 4 M solution for 50 min. (b) Charge-discharge curves of the dealloyed samples. The charge-discharge current density is 6 mA cm^{-2}. Inset shows the V_{drop} in discharge process. (c) The areal specific capacitance of $Al_{85-x}Ni_6Y_6Co_3Cu_x$ (x = 1, 3 and 5) dealloyed 50 min as a function of copper content. (d) The ESR of $Al_{85-x}Ni_6Y_6Co_3Cu_x$ (x = 1, 3 and 5) dealloyed 50 min as a function of copper content. Inset shows the V_{drop} versus the concentration of Cu at different current densities at room temperature in 4 M KOH.

that the specific capacitance of the de-alloyed $Al_{85-x}Ni_6Y_6Co_3Cu_x$ (x = 1, 3, 5) are 1.06, 1.22 and 0.77 F cm^{-2}, respectively, as shown in Fig. 3c.

The equivalent series resistance (ESR) during charging and discharging was studied for the materials with different compositions. As shown in the inset of Fig. 3b, the voltage drop (V_{drop}) in the discharge curve was proportional to the ESR. The ESR is composed of several resistive phenomena: resistance of electrolyte, resistance from charge-transfer reaction and electrical conduction within electrode. For the same electrolyte, the ESR is a combination of the resistances from charge-transfer reaction and electrode. As shown in the inset of Fig. 3d, the de-alloyed $Al_{82}Ni_6Y_6Co_3Cu_3$ exhibits the smallest V_{drop} compared to the other two compositions, which denotes the best electric conductance in comparison. The ESR is estimated to be about 16.0, 8.4 and 45.3 Ω cm^{-2} for x = 1, 3, 5 according to the slope in the inset of Fig. 3d. Above all, adding Cu by 3 at. % can enhance the capacitance by decreasing the electric resistance.

On the other hand, the de-alloying time and the concentration of electrolyte are also key factors for the electrochemical performance of nanoporous materials. It is in need to figure out the optimal parameters. Firstly, to study the effect of de-alloying time on electrochemical properties, the $Al_{82}Ni_6Y_6Co_3Cu_3$ glassy precursor was de-alloyed in 4 M KOH solution for various time. Fig. 4a shows the cyclic voltammetry (CV) curves of the de-alloyed sample evaluated as a binder-free electrode in different de-alloying time at the scan rate of 10 mv s^{-1}. In the CV curves, the broad peaks in the region between 0.2 and 0.45 V (vs Ag/AgCl) correspond to the Faradic redox reactions of Ni and Co oxides/hydroxides [21,22]. At the same scan rates, the current intensities increase with the increasing de-alloying time, indicating the higher integral area of the CV curve. Fig. 4b shows GCD curves of the de-alloyed $Al_{82}Ni_6Y_6Co_3Cu_3$ glassy precursor in different de-alloying time at the current density of 6 mA cm^{-2}. Along with the de-alloying time,

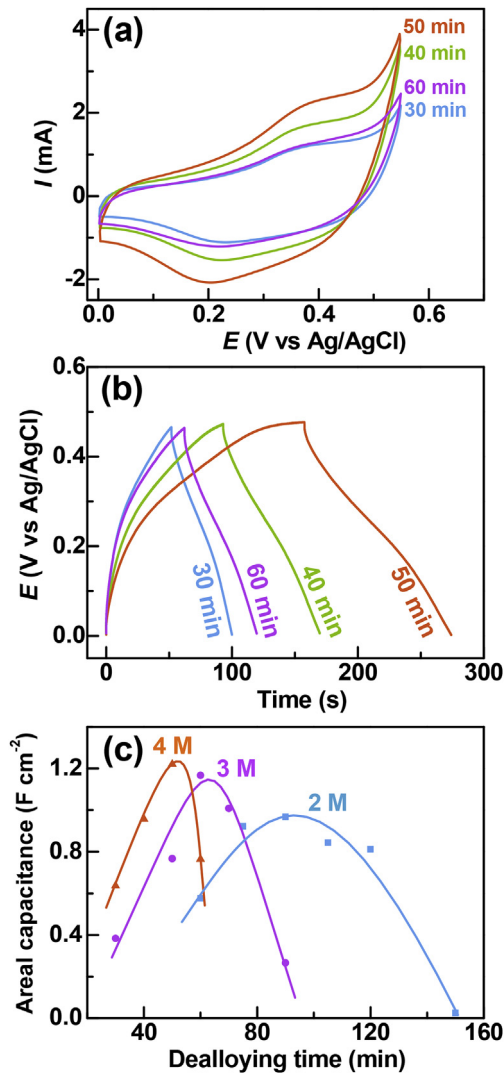in Fig. 5. The ligaments of the nanoporous structure become much thinner when being de-alloyed at solutions with high concentration of KOH. Because the thickening of ligaments is controlled by the diffusion of metallic elements [23] and the de-alloying reaction is much faster in solutions with higher concentrations, the formation of thinner ligament is attributed to the less diffusion time during de-alloying. Such thin ligaments provide large specific surface area.

The electrode of $Al_{82}Ni_6Y_6Co_3Cu_3$ precursors de-alloyed in 4 M KOH for 50 min not only has biggest specific capacitance (1.221 F cm^{-2} at 6 mA cm^{-2}) in those three $Al_{85-x}Ni_6Y_6Co_3Cu_x$ (x = 1, 3 and 5) composition, but also is better than previously reported value for such free-standing electrodes, such as Co_3O_4@RuO_2 nanosheet arrays (0.86 F cm^{-2} at 10 mA cm^{-2}) [24], Co_3O_4@MnO_2 NW/nanosheet core-shell arrays (0.56 F cm^{-2} at 11.25 mA cm^{-2}) [25], NiO/Ni nanowire arrays (0.36 F cm^{-2} at 5 mA cm^{-2}) [26], and NiO nanoflake arrays (0.25 F cm^{-2} at 2 A g^{-1}) [27]. More literature results are summarized in Table 1. This good electrochemical performance could be related to the following structural features. Firstly, the continuous nanoporous structure leads to a high surface area which undoubtedly contributes to the

Fig. 4. (a) CV curves of dealloyed $Al_{82}Ni_6Y_6Co_3Cu_3$ alloy at scanning rate of 10 mV s^{-1}. (b) Charge-discharge curve of dealloyed $Al_{82}Ni_6Y_6Co_3Cu_3$ at current density of 6 mA cm^{-2}. (c) The area specific capacitance of dealloyed $Al_{82}Ni_6Y_6Co_3Cu_3$ at different concentration of the etching solutions as a function of dealloying time.

the electrochemical charging-discharging capacity increases to about 1.22 F cm^{-2} for 50 min and then decrease if it is de-alloyed for longer time (i.e. 60 min). The increase of capacity till 50 min is attributed to the growth in the thickness of nanoporous NiCo metal/oxides, which indicates more active materials for charging-discharging reactions. However, upon further de-alloying, the electric conductivity will decrease if there are too much of oxides.

To study the influence of the concentration of electrolytes, the electrochemical capacitance of the sample de-alloyed in electrolytes with different concentration of KOH is shown in Fig. 4c. It took more de-alloying time to reach the highest capacitance for the diluted solutions. The optimum de-alloying time is 50, 60 and 90 min for 2 M, 3 M and 4 M solutions, respectively. The maximum capacitance also depends on the solution concentration. When being de-alloyed at solutions with higher concentration, the capacitance becomes larger at the optimum de-alloying time, but the time window for obtaining a better capacitance becomes narrow.

To gain insights into effects of the etching solution concentration on the nanoporosity, we studied the micro-structure of the optimum de-alloyed samples in different KOH solutions, as shown

Fig. 5. SEM images of the surfaced for the $Al_{82}Ni_6Y_6Co_3Cu_3$ metallic glass dealloyed for 50 min in KOH solutions with different concentrations, (a) 2 M, (b) 3 M, (c) 4 M, respectively.

Table 1
Comparison of the capacitance of the continuous nanoporous metal/metal-oxide composites with literature results.

Electrode	Performance F cm^{-2}	Current density mA cm^{-2}	Refs
np-Ni-Co metal/metal-oxide	1.22	6	This work
Co$_3$O$_4$@MnO$_2$ NW/nanosheet core-shell arrays	0.4–0.7	11.25	[25]
Ni-NiO core-shell inverse opal	0.0078–0.009	0.2	[28]
CNT/Ni hybrid nanostructured arrays	0.901	0.69	[29]
Co$_3$O$_4$ nanowire arrays	0.6–0.68	4	[27]
NiO nanoflake arrays	0.2–0.25	4	[27]
Coaxial Nio/Ni nanowire arrays	0.36–0.365	5	[26]
MnO$_2$-NiO tubular arrays	0.4	5	[30]
Co$_9$S$_8$ nanorod arrays	0.84–0.86	10–50	[22]
np-YNiCo metal/metal-oxide	1.12	2	[31]
Hierarchical np-Ni alloy	1.11	1.25	[32]

high capacitance. Secondly, the nanoporous structure supports more active sites and facilitates the mass transfer which contributes to the high capacitance. Thirdly, the doping of copper decreases the equivalent series resistance which results in smaller internal resistance of the electrode materials.

4. Conclusions

In summary, nanoporous NiCo metal/metal-oxide composites have been fabricated successfully by one-step de-alloying Al$_{85-x}$Ni$_6$Y$_6$Co$_3$Cu$_x$ metallic glass precursors. Alloying of noble metal (Cu) is beneficial for increasing electrochemical capacitance by decreasing the electric resistance of the composite. Dealloying the Al$_{82}$Ni$_6$Y$_6$Co$_3$Cu$_3$ sample in 4 M KOH for 50 min can achieve the largest areal specific capacitance 1.22 F cm^{-2} at 6 mA cm^{-2}. These results suggest that AlNiCo-based metallic glasses are promising candidates as precursors for fabricating metal/metal-oxides composites with homogeneous nanoporosity and hold promising application potential as binder-free electrodes. The fabrication strategy is applicable for mass production and provides a good opportunity for fabrication of various kinds of functional nanoporous metals which may be useful in energy storage.

Acknowledgements

References

[1] M. Winter, R.J. Brodd, What are batteries, fuel cells, and supercapacitors? Chem. Rev. 104 (2004) 4245–4269.

[2] Y. Wang, Z.Q. Shi, Y. Huang, Y.F. Ma, C.Y. Wang, M.M. Chen, Y.S. Chen, Supercapacitor devices based on graphene materials, J. Phys. Chem. C 113 (2009) 13103–13107.

[3] Y. Zhang, H. Feng, X. Wu, L. Wang, A. Zhang, T. Xia, H. Dong, X. Li, L. Zhang, Progress of electrochemical capacitor electrode materials: a review, Int. J. Hydrogen Energy 34 (2009) 4889–4899.

[4] Y. Gogotsi, P. Simon, True performance metrics in electrochemical energy storage, Science 334 (2011) 917–918.

[5] G. Wang, L. Zhang, J. Zhang, A review of electrode materials for electrochemical supercapacitors, Chem. Soc. Rev. 41 (2012) 797–828.

[6] M. Beidaghi, Y. Gogotsi, Capacitive energy storage in micro-scale devices: recent advances in design and fabrication of micro-supercapacitors, Energy Environ. Sci. 7 (2014) 867.

[7] A.G. Pandolfo, A.F. Hollenkamp, Carbon properties and their role in supercapacitors, J. Power Sources 157 (2006) 11–27.

[8] P. Simon, Y. Gogotsi, Materials for electrochemical capacitors, Nat. Mater 7 (2008) 845–854.

[9] M. Salanne, B. Rotenberg, K. Naoi, K. Kaneko, P.L. Taberna, C.P. Grey, B. Dunn, P. Simon, Efficient storage mechanisms for building better supercapacitors, Nat. Energy 1 (2016) 16070.

[10] X.Y. Lang, A. Hirata, T. Fujita, M.W. Chen, Nanoporous metal/oxide hybrid electrodes for electrochemical supercapacitors, Nat. Nanotechnol. 6 (2011) 232–236.

[11] H.J. Jin, X.L. Wang, S. Parida, K. Wang, M. Seo, J. Weissmuller, Nanoporous Au-Pt alloys as large strain electrochemical actuators, Nano Lett. 10 (2010) 187–194.

[12] R. Wang, C. Wang, W.B. Cai, Y. Ding, Ultralow-platinum-loading high-performance nanoporous electrocatalysts with nanoengineered surface structures, Adv. Mater. 22 (2010) 1845–1848.

[13] L.Y. Chen, Y. Hou, J.L. Kang, A. Hirata, M.W. Chen, Asymmetric metal oxide pseudocapacitors advanced by three-dimensional nanoporous metal electrodes, J. Mater. Chem. A 2 (2014) 8448–8455.

[14] F. Cai, Y. Kang, H. Chen, M. Chen, Q. Li, Hierarchical CNT@NiCo$_2$O$_4$ core–shell hybrid nanostructure for high-performance supercapacitors, J. Mater. Chem. A 2 (2014) 11509.

[15] D.S. Patil, J.S. Shaikh, S.A. Pawar, R.S. Devan, Y.R. Ma, A.V. Moholkar, J.H. Kim, R.S. Kalubarme, C.J. Park, P.S. Patil, Investigations on silver/polyaniline electrodes for electrochemical supercapacitors, Phys. Chem. Chem. Phys. 14 (2012) 11886–11895.

[16] G.Q. Zhang, H.B. Wu, H.E. Hoster, M.B. Chan-Park, X.W. Lou, Single-crystalline NiCo$_2$O$_4$ nanoneedle arrays grown on conductive substrates as binder-free electrodes for high-performance supercapacitors, Energy Environ. Sci. 5 (2012) 9453.

[17] S.J. Zhu, J.Q. Jia, T. Wang, D. Zhao, J. Yang, F. Dong, Z.G. Shang, Y.X. Zhang, Rational design of octahedron and nanowire CeO$_2$@MnO$_2$ core-shell heterostructures with outstanding rate capability for asymmetric supercapacitors, Chem. Commun. 51 (2015) 14840–14843.

[18] J. Kang, A. Hirata, L. Kang, X. Zhang, Y. Hou, L. Chen, C. Li, T. Fujita, K. Akagi, M. Chen, Enhanced supercapacitor performance of MnO$_2$ by atomic doping, Angew. Chem. 52 (2013) 1664–1667.

[19] D.V. Louzguine, A. Inoue, Investigation of structure and properties of the Al-Y-Ni-Co-Cu metallic glasses, J. Mater. Res. 17 (2002) 1014–1018.

[20] R. Li, X.J. Liu, H. Wang, D.Q. Zhou, Y. Wu, Z.P. Lu, Formation mechanism and characterization of nanoporous silver with tunable porosity and promising capacitive performance by chemical dealloying of glassy precursor, Acta Mater. 105 (2016) 367–377.

[21] V. Gupta, S. Gupta, N. Miura, Potentiostatically deposited nanostructured Co$_x$Ni$_{1-x}$ layered double hydroxides as electrode materials for redox-supercapacitors, J. Power Sources 175 (2008) 680–685.

[22] J. Zhang, H. Gao, Q. Yang, X.T. Zhang, M.Y. Zhang, L.L. Xu, Effect of temperature on pseudocapacitance performance of carbon fiber@NiCo$_2$O$_4$@Ni(OH)$_2$ core-shell nanowire array composite electrodes, Appl. Surf. Sci. 356 (2015) 167–172.

[23] R. Li, X.J. Liu, H. Wang, Y. Wu, X.M. Chu, Z.P. Lu, Nanoporous silver with tunable pore characteristics and superior surface enhanced Raman scattering, Corros. Sci. 84 (2014) 159–164.

[24] J. Xu, Q.F. Wang, X.W. Wang, Q.Y. Xiang, B. Hang, D. Chen, G.Z. Shen, Flexible asymmetric supercapacitors based upon Co$_9$S$_8$ nanorod//Co$_3$O$_4$@RuO$_2$ nanosheet arrays on carbon cloth, Acs Nano 7 (2013) 5453–5462.

[25] J. Liu, J. Jiang, C. Cheng, H. Li, J. Zhang, H. Gong, H.J. Fan, Co$_3$O$_4$ Nanowire@MnO$_2$ ultrathin nanosheet core/shell arrays: a new class of high-performance pseudocapacitive materials, Adv. Mater 23 (2011) 2076–2081.

[26] M. Hasan, M. Jamal, K.M. Razeeb, Coaxial NiO/Ni nanowire arrays for high performance pseudocapacitor applications, Electrochim. Acta 60 (2012) 193–200.

[27] X.H. Xia, J.P. Tu, Y.Q. Zhang, X.L. Wang, C.D. Gu, X.B. Zhao, H.J. Fan, High-quality metal oxide core/shell nanowire arrays on conductive substrates for electrochemical energy storage, Acs Nano 6 (2012) 5531–5538.

[28] J.H. Kim, S.H. Kang, K. Zhu, J.Y. Kim, N.R. Neale, A.J. Frank, Ni-NiO core-shell inverse opal electrodes for supercapacitors, Chem. Commun. 47 (2011) 5214–5216.

[29] J. Jiang, J. Liu, W. Zhou, J. Zhu, X. Huang, X. Qi, H. Zhang, T. Yu, CNT/Ni hybrid nanostructured arrays: synthesis and application as high-performance electrode materials for pseudocapacitors, Energy Environ. Sci. 4 (2011) 5000.

[30] J.P. Liu, J. Jiang, M. Bosman, H.J. Fan, Three-dimensional tubular arrays of MnO$_2$-NiO nanoflakes with high areal pseudocapacitance, J. Mater. Chem. 22 (2012) 2419–2426.

[31] H.J. Qiu, Y. Ito, M.W. Chen, Hierarchical nanoporous nickel alloy as three-dimensional electrodes for high-efficiency energy storage, Scr. Mater. 89 (2014) 69–72.

[32] H.J. Qin, J.Q. Wang, P. Liu, Y. Wang, M.W. Chen, Hierarchical nanoporous metal/metal-oxide composite by dealloying metallic glass for high-performance energy storage, Corros. Sci. 96 (2015) 196–202.